Intracellular screening of a peptide library to derive a potent peptide inhibitor of α-synuclein aggregation.

Harish Cheruvara[1], Victoria L Allen-Baume[1], Neil M Kad,[2,4], and Jody M Mason[3,4]

[1]School of Biological Sciences, University of Essex, Wivenhoe Park, Colchester, Essex, CO4 3SQ

[2]School of Biosciences, University of Kent, Canterbury, Kent, CT2 7NJ

[3]Department of Biology and Biochemistry, University of Bath, Claverton Down, Bath, BA2 7AY

[4]These authors contributed equally to this work

[1]To whom correspondence should be addressed: j.mason@bath.ac.uk

Running title: Intracellular selection of an α-synuclein aggregation inhibitor

Keywords: amyloid, protein misfolding, protein-protein interactions, library screening, protein-fragment complementation assay, Parkinson's disease, α-synuclein

Background: Deposition of α-syn into Lewy Bodies is considered the primary event in Parkinson's disease.
Results: A peptide selected via PCA library screening functions by inhibiting fibril formation
Conclusion: Semi-rational design combined with intracellular PCA is an effective methodology to develop α-syn aggregation antagonists
Significance: The technique can be applied to a number of diseases from Parkinson's to Alzheimer's.

ABSTRACT

Aggregation of α-synuclein (α-syn) into toxic fibrils is a pathogenic hallmark of Parkinson's disease (PD). Studies have largely focused on residues 71-82, yet most early onset mutations are located between residues 46-53. A semi-rationally designed 209,952 member library based entirely on this region was constructed, containing all wild-type residues and changes associated with early onset PD. Intracellular cell-survival screening and growth competition isolated a 10-residue peptide antagonist that potently inhibits α-syn aggregation and associated toxicity at 1:1 stoichiometry. This was verified using continuous growth measurements, and MTT cytotoxicity studies. Atomic force microscopy and circular dichroism on the same samples showed a random-coil structure and no oligomers. A new region of α-syn for inhibitor targeting has been highlighted, together with the approach of using semi-rational design and intracellular screening. These peptides are candidates for modification into drugs capable of slowing or even preventing the onset of PD.

Deposition of α-synuclein (α-syn) into neuronal inclusions known as Lewy bodies is considered the causative agent in the pathogenesis of Parkinson's disease (PD), a debilitating disease which results principally in rigidity, tremor and slowness of movement and accounts for approximately 15% of all dementias (1,2). The accumulation of toxic

Lewy bodies in the cytoplasmic space of dopaminergic neurons in the substantia nigra pars compacta region of the brain leads to cell death, decreased dopamine levels, and ultimately the symptoms of the disease. There is a substantial and growing body of evidence implicating α-syn in PD (3), including: i) synthetic α-syn rapidly aggregates into β-sheet rich fibrils similar to those found in Lewy bodies; ii) rare familial mutations that increase fibril aggregation rates and toxicity lead to early onset PD; iii) α-syn gene duplications lead to increased protein expression and therefore accelerate disease onset, and iv) α-syn oligomers are toxic to therapeutically relevant cells in culture. To intervene in PD we have utilised a novel intracellular screen to identify peptides capable of binding to and reducing the associated toxicity of a-syn aggregation. Our approach has the potential to address recent findings that suggest that pre-fibrillar oligomers are the toxic species (4).

There is a wealth of experimental data demonstrating that region 71-82 is responsible for the aggregation of the full length 140 amino acid protein(5-7). Indeed, numerous groups have used this region as a starting point for the design of inhibitors. This has included non-modified peptides (8) and N-methylated peptides (9). Given the interest in this region and its requirement for aggregation of the full-length protein, many groups have focused their efforts on producing libraries based on this scaffold. However, of the known point mutations in the α-syn gene associated with early onset PD, three (E46K, H50Q, A53T) are located between residues 46-53 with the fourth (A30P) located in close proximity. More recently a fifth mutation, G51D, has been identified (10). This region and the residues within are clearly important in modulating amyloid formation such that toxicity associated with the α-syn protein becomes increased, with the changes leading to decreased α-helicity, increased β-sheet propensity, and either an increase in the rate or in the number of oligomers that are formed (11-14).

Here we have generated peptide inhibitors using a multiplexed intracellular *Protein-fragment Complementation Assay* (PCA) library screening system (15,16) followed by direct imaging of the samples. Successfully selected peptides must bind α-syn to reduce amyloid cytotoxicity and confer bacterial cell survival. During PCA no assumptions are therefore made regarding the mechanism of action or the oligomeric state of α-syn that becomes populated. The only prerequisite for peptide selection is that ***i)*** peptides bind to α-syn such that the split reporter enzyme is recombined and ***ii)*** that the result is lower toxicity such that cell survival is facilitated. In addition, the PCA approach is predicted to select peptides that are resistant to degradation by bacterial proteases, to be soluble, non-toxic, and to be target specific in the presence of other cytoplasmic proteins.

Using α-syn$_{45-54}$ as a template for our library design we have created a 209,952 member peptide library ten amino acids in length that spans residues 45-54 containing the wild-type 45-54 sequence, including residue options corresponding to E46K, H50Q, and A53T which when mutated give rise to early-onset PD. PCA has been used to screen the peptide library for an interaction with wild-type α-syn. The effectiveness of an amyloid-PCA selected peptide has been subsequently tested by performing four key experiments upon the same sample. These experiments are a continuous amyloid growth assay, monitored using ThT fluorescence, circular dichroism, to report on changes in β-sheet content, and atomic force microscopy and SDS-PAGE analysis, to directly image any reduction in fibril load and changes in the fibril morphology. We find the peptide derived using this approach to be capable of binding to the disease relevant wild-type α-syn and reducing associated amyloid formation by over 90%. This study has both successfully verified the methodology for producing anti α-syn aggregation peptide inhibitors using the amyloid-PCA approach as well as produced a lead peptide sequence that is expected to provide a scaffold for future drug candidates.

Our data collectively indicate that the PCA derived 45-54W sequence is able to prevent the aggregation of wild-type α-syn at a stoichiometry of 1:1. The ThT fluorescence signal associated with amyloid formation does not progress beyond ~8% of the original 1:0 sample. Atomic force microscopy experiments show that in the same continuous growth samples there is a striking loss in the number of fibrils relative to the 1:0 samples. MTT

cytotoxicity studies using the same samples show a reduction in cell death of 65-85% compared to α-syn in isolation. Finally, circular dichroism experiments using samples taken from the same continuous growth experiment once again show that the conversion from a random coil structure to a β-sheet rich structure is almost completely abolished in the 1:1 sample. At a molar ratio of 1:0.5 the formation of the mature amyloid fibrils found in the 1:0 is slowed but ultimately not prevented (see Figure 3a). At stoichiometries of 1:0.1 and 1:001 the rate of amyloidosis is not significantly lowered relative to the 1:0 sample.

EXPERIMENTAL PROCEDURES

Primers and library cloning: Primers were designed such that the desired library could be generated using overlap-extension PCR. Bases overlapped in a non-randomised region of the primers to give an approximate annealing temperature of 66°C. Correct amplification was enabled via an elongated reverse primer and verified by agarose gel electrophoresis. The correct PCR product was then digested using NheI and AscI restriction enzymes for subcloning of the library into the pES230d vector (restriction enzyme recognition sites shown). Primer sequences used were: Forward Primer: 5'- C TGG GCT AGC RAA VAW GBG VTT VTT VAW GBG VTT RHA RCC GGC GCG CCG CTA GAG GCG -3'; Reverse Primer: 5'- T TTT TTT TTA TAA TAT ATT ATA CGC CTC TAG CGG CGC GCC -3'. An additional 30 residues on the 5' end of the reverse primer was used to observe the correct PCR product prior to restriction digestion.

Single Step Selection PCA – *E.coli* XL-1 cells were used for construction and cloning of libraries as described previously (16-18). Firstly pES300d–α-syn target and pREP4 (Qiagen; for expression of the lac repressor protein) were co-transformed into BL-21 gold cells (Stratagene) and plated onto LB agar with the appropriate antibiotics (Kan and Cm). These cells were next made electrocompetent before transformation with pES230d–45-54 library plasmid. Transformed cells were plated onto three different media; $1/20^{th}$ of the cells were plated onto LB agar with three antibiotics (Kan, Amp, and Cm) as a positive control of transformation efficiency. A further $1/20^{th}$ of the solution was plated onto M9 minimal medium agar containing 1μg/ml trimethoprim and the same three antibiotics as a negative control. Finally, the remaining 90% of transformed cells were plated onto M9 minimal agar in the presence of the three antibiotics, 1μg/ml trimethoprim, and 1 mM IPTG (isopropyl-β-D-thiogalactopyranoside), to induce expression of the two DHFR fragment fused peptides). This single-step PCA selection led to approximately 200 colonies from the initial library of 209,952 meaning that >99.9% of all library members are removed at this stage owing to their inability to bind α-syn.

Competition Selection PCA - To increase selection stringency, growth competition experiments were undertaken. Selected colonies were pooled from the plate and grown in M9 minimal media under selective conditions (containing Kan, Amp, Cm, trimethoprim and IPTG) and serially diluted over 5 passages (p1-p5). Using these sequential rounds of competition selection, subtle differences in growth rate can become amplified, increasing the stringency of selection relative to the single-step method. Competition selection therefore allows the most effective 1-2 sequences to be isolated from the ~200 α-syn binders initially identified during single step selection. At each passage glycerol stocks were prepared and sequencing results were obtained (Source bioscience, Nottingham) for DNA pools as well as individual colonies. For each passage, 50 μl of liquid culture was added to 50 ml of fresh M9 minimal media, resulting in an approximate OD_{600} of 0.01. Cells were incubated at 37°C until an OD_{600} of ~0.4 was reached (typically 2-3 days), before moving to the next passage.

Protein expression and purification – Wild-type α-syn was synthesized by overexpression in *E.coli* (BL21) strain using a small ubiquitin related modifier (SUMO) fusion (19). SUMO modulates protein structure and function by covalently binding to the lysine side chains of the target protein to enhance expression and solubility of the α-syn protein. *E.coli* BL21 competent cells were transformed with pET21b plasmid construct and grown on Luria Bertani (LB) plates containing Amp and Cm and grown overnight. Single colonies were next picked,

inoculated in LB broth containing Amp and Cm and shaken at 37°C. These cultures were then used to inoculate 2 litres of liquid Luria broth containing Amp and Cm and grown to the mid log phase growth (OD_{600} = 0.6-0.8) before being further induced by 1mM IPTG for 3 hours at 37°C. Cells were obtained by centrifugation at 4000rpm 20 minutes at 4°C in a Sorvall RC superspeed centrifuge. Cell pellets were then resuspended in binding buffer (50 mM NaH_2PO_4, 300 mM NaCl, 10 mM imidazole, pH: 8) and homogenised using a magnetic stirrer for 15 minutes on ice followed by sonication (40% amplification). Lysed cells were next centrifuged at 18,500 rpm for 20 mins at 4°C using an SS-34 rotor (Sorvall RC superspeed centrifuge). The supernatant containing the protein was stored at -20°C.

Purification of the fusion protein was achieved by applying the supernatant from the cell lysate on to an Ni-NTA affinity column at a flow rate of 3 mL/min three times to allow the protein to bind. The column was next washed with 40 mL wash buffer (50 mM NaH_2PO_4, 300 mM NaCl, 30 mM imidazole, pH: 8) and the protein was eluted using elution buffer (50mM NaH_2PO_4, 300mM NaCl, 500 mM imidazole, pH: 8). The protein sample was then exchanged to cleavage buffer (20 mM Tris, 0.5 mM DTT, pH 8.0) using a PD10 desalting column. The ^{6}His-SUMO tag was removed using specific SUMO protease-UlP1 enzyme (1mg/mL for 10mg/mL of target protein) at 30°C for 16 hours.

The ^{6}His-SUMO was finally removed using a size-exclusion column. G-75 column was washed 3 times with 10mM MES, 150 mM NaCl, pH 8.0. The protein was concentrated to 2mL, injected to the column and fractions were eluted according to their molecular weight. Finally, SDS-PAGE was used to determine the purity of the α-syn and to verify that the expected molecular mass different fractions containing α-syn (14.7 kDa), SUMO protein (12.2 kDa), and SUMO protease (27 kDa). The correct mass of α-syn was further confirmed using electro-spray mass spectrometry. The protein concentration was finally determined in a Varian cary-50 spectrophotometer. The purified protein was lyophilized using a freeze drier and stored at -80^{0}C.

Monomerisation of Protein for aggregation studies - In order to monomerise the protein prior to aggregation experiments; 1mL of hexafluoro-2-propanol (HFIP) was added to 2mg of lyophilized peptide. This was next vortexed for approximately 2 minutes to fully dissolve the peptide, followed by sonication at 25^{0}C for 5 minutes in a water bath sonicator. HFIP was allowed to evaporate completely under a regulated stream of air. The process was repeated 3 times, followed by dissolution of peptide sample in double distilled water, vortexing for 3 minutes and lyophilization for further use (9).

Peptide synthesis – Rink amide ChemMatrixTM resin was obtained from PCAS Biomatrix, Inc. (St.-Jean-sur-Richelieu, Canada); Fmoc-l-amino acids and 1H-Benzotriazol-1-yloxy)(dimethylamino)-N,N-dimethylmethaniminium hexafluorophosphate (HBTU) were obtained from AGTC Bioproducts (Hessle, UK); all other reagents were of peptide synthesis grade and obtained from Thermo Fisher Scientific (Loughborough, UK). Peptide 45-54W was synthesized on a 0.1-mmol scale on a PCAS Biomatrix^{TM} Rink amide resin using a Liberty Blue^{TM} microwave peptide synthesizer (CEM; Matthews, NC) employing Fmoc solid-phase techniques (for review see (20)) with repeated steps of coupling and deprotection and washing (4 × 5 ml dimethylformamide). Coupling was performed as follows: Fmoc amino acid (5 eq), HBTU (4.5 eq), and diisopropylethylamine (10 eq) in dimethylformamide (5 ml) for 5 min with 20-watt microwave irradiation at 90°C. Deprotection was performed as follows: 20% piperidine in dimethylformamide for 5 min with 20-watt microwave irradiation at 80°C. Following synthesis, the peptide was acetylated (acetic anhydride (3 eq) and diisopropylethylamine (4.5 eq) in dimethylformamide (2.63 ml) for 20 min) and then cleaved from the resin with concomitant removal of side chain-protecting groups by treatment with a cleavage mixture (10 ml) consisting of TFA (95%), triisopropylsilane (2.5%), and H_2O (2.5%) for 4 h at room temperature. Suspended resin was removed by filtration, and the peptide was precipitated using three rounds of crashing in ice-cold diethyl ether, vortexing and centrifugation. The

pellet was then dissolved in 1:1 MeCN/H_2O and freeze-dried. Purification was performed by RP-HPLC using a Phenomenex Jupiter Proteo (C12) reverse phase column (4 μm, 90 Å, 10 mm inner diameter × 250 mm long). Eluents used were as follows: 0.1% TFA in H_2O (A) and 0.1% TFA in MeCN (B). The peptide was eluted by applying a linear gradient (at 3 ml/min) of 20% to 60% B over 40 min. Fractions collected were examined by electrospray mass spectrometry, and those found to contain exclusively the desired product were pooled and lyophilized. Analysis of the purified final product by RP-HPLC indicated a purity of >95%.

Peptide preparation - Stock solutions of 1mM concentration of the inhibitor and control peptides were dissolved in ultrapure water. At this concentration, a 2-200 fold excess of that used in experiments, no aggregation or precipitate was observed. In addition, bioinformatics tools (e.g. Waltz (21), Amylpred (22), Pasta (23), Zyggregator (24), and Tango (25)) did not predict the peptide to contain amyloidogenic sequences or aggregate in isolation. Lastly dye-binding experiments demonstrate that this sequence does not bind ThT or aggregate and form random-coil like species in isolation using CD (Figures 3 and 4).

Continuous growth ThT Experiments - The provided winner was lyophilized in the molar concentration of target protein and inhibitory peptide as 1:1. The reaction mixture containing 450μM wild-type α-syn and inhibitory peptide was incubated in 90μM ThT, 10mM Phosphate buffer (pH 7.0), 100mM KF and 0.05% NaN3 at 37^0C with continuous mixing using a magnetic flea in an LS55 fluorescence spectrophotometer (Perkin Elmer) for 4500 minutes (75 hours). The same experiment was repeated three times for both 1:0 and for 45-54W containing solutions at a variety of stoichiometries, as well as 1:1 molar ratios with the control peptides 45-54wt and 71-82W. The PCA winner 45-54 peptide was lyophilized in aliquots of different molar concentrations of target protein and inhibitory peptide ranging from 1:0.01, to 1:1.

Circular Dichroism Experiments - Far-UV circular dichroism (CD) spectra were recorded on an Applied Photophysics Chirascan at 20 °C using the same samples from the continuous growth ThT experiments. Spectra were recorded over the 200-300 nm range at a scan rate of 10 nm/min with step size of 1 nm. Spectra were recorded as the average of three scans. Peptide (10 μM in 10 mM Potassium Phosphate buffer pH 7.4) was added to a 0.1 cm cuvette (Hellma). Spectra were recorded as raw ellipticity.

Atomic force microscopy experiments - Samples were imaged in noncontact mode using a XE- 120 Atomic Force Microscope (Park Systems, South Korea). NSC 15 silicon nitride cantilevers with a spring constant of 40 N/m were used for imaging at a scan rate of 1.0 Hz and a resolution of 256 x 256 pixels. All images were taken at room temperature. The AFM data were taken from continuous growth experiments. A 5 μL sample was taken from the 450 μM α-syn continuous growth experiment and placed on freshly cleaved mica (thickness 0.3 mm). Following adsorption of the protein aggregates (2 min), the mica was washed with 5 mL of double distilled water. Excess water was removed and the samples were dried using a stream of nitrogen gas. Samples were immediately analyzed by AFM. The image files were examined using WSxM v5.0 (Nanotec Electronica S.L.) and flattened before processing (26).

3-(4,5.Dimethylthiazol-2-yl)-2,5-diphenyltetrazolium Bromide (MTT) Cell-Toxicity Assay - MTT experiments were undertaken using Rat phaeochromocytoma (PC12) cells to assess cytotoxicity effect of α-syn. PC12 cells are known to be particularly sensitive and their use in this assay is well established (27). The MTT Vybrant® MTT Cell Proliferation Assay Kit (Invitrogen) was used to measure the conversion of the water soluble MTT dye to formazan, which is then solubilized, and the concentration determined by a purple colour change monitored via absorbance measurement at 570 nm. The change in absorbance can be used as an indicator of the PC12 cell health in the assay. The assay was performed with 5 μM α-syn and peptide stoichiometry corresponding to 1:1 (5 μM). PC12 cells were maintained in RPMI 1640 +2mM glutamine medium mixed with

10% horse serum, 5% foetal bovine serum, supplemented with a 20mg/mL gentamycin. Cells were transferred to a sterile 96-well plate with 30,000 cells per well and experiments performed in triplicate. A required volume of peptide and target solutions was added to PC12 cells. A total of 100 µL of PC12/RPMI media combined with an appropriate volume of peptide/ α-syn target mixture (5 µM peptide + 5µM α-syn target) was transferred to a 96 well microtitre plate. Since the samples contain 90µM ThT, controls of PC12 cells and α-syn alone, both with and without ThT were undertaken. These were incubated for 24 h at 37 °C, 5% CO_2, prior to the addition of the MTT dye. A total of 10 µL of the dye was added to each well and incubated for a further 4h at 37 °C, 5% CO_2. A total of 100 µL of the DMSO was then added to each well and was allowed to stand for 10 minutes. The absorbance was measured at 570 nm using a Berthold Tristar LB942 plate reader.

SDS-PAGE – Gel analysis was carried out using 15% Tris-bis acrylamide gels operated at a constant voltage of 150 V. The running buffer was 25mM Tris-HCl, 193 mM glycine, and 0.1% SDS (pH 8.3). 3 µL of 450 µM α-syn along with peptides at different stoichiometries were mixed with 7 µL of loading buffer containing 50 mM Tris-HCl (pH 6.8), 1% SDS, 5% glycerol, and 25% bromophenol blue. 10 µL of each sample was then loaded in each well. The gel was stained using 0.1% Coomassie blue R250.

RESULTS

α-syn 45-54 library generation – PCA was undertaken with full length α-syn_{1-140} target using a library based on the α-syn_{45-54} region in which three of the four α-syn mutations associated with early onset PD are located (KEGVVHGVAT; wild-type 45-54). Unlike α-syn_{71-82}, this is not a region of the molecule known to aggregate into toxic fibrils in isolation (28-30) and therefore has not been exploited as a starting point for deriving α-syn binders capable of inhibiting aggregation. The library incorporated the wild-type sequence while introducing two, three or six residue options at each of the ten amino acid positions (see Figure 1). This corresponded to a library size of 209,952. Single step selection on M9 plates was undertaken followed by competition selection in M9 liquid media, resulting in one clean sequencing result by passage six; KDGIVNGVKA (Figure 2).

Peptide characterization – PCA derived peptide sequences (Figure 1) were synthesized and characterised using a number of experiments that included thioflavin-T (ThT) dye binding, circular dichroism (CD), atomic force microscopy (AFM), and MTT cytotoxicity experiments in order to verify if the peptides do not aggregate in isolation and if they are able to reduce aggregation and/or breakdown preformed fibrils to a non-toxic species.

Continuous growth ThT experiments demonstrate a significant reduction in fibril load – To determine the ability of PCA derived peptides to reduce fibril assembly (inhibition) and/or breakdown preformed fibrils (reversal), ThT binding was used to quantify amyloid species. Firstly, α-syn was rendered monomeric (9) and aggregated into amyloid by resuspending and incubating at 37°C. For the continuous growth assay, peptides were added at time zero and a reading taken every five minutes over a 75 hour period. The ThT signal was significantly reduced at a 1:1 molar ratio indicating that the peptides is able to bind α-syn and reduce aggregation levels. At increasingly lower sub-stoichiometric ratios, we observed progressively reduced activity consistent with a general dose dependency. The control peptide 71-82W as well as the wild-type 45-54 sequence at 1:1 molar rations had no effect upon aggregation demonstrating α-syn specificity for the 45-54W peptide.

Atomic Force Microscopy indicates a large reduction in amyloid levels – As a second direct qualitative measure of fibril formation samples used in continuous growth experiments were imaged using AFM (Figure 3b-f). A stoichiometry of 1:1 (450 µM:450 µM) was chosen for AFM experiments as this was found to be the most effective in ThT experiments (Figure 3b). At this stoichiometry a major reduction in the amount of amyloid was observed relative to the α-syn control across several time points (Figure 3d). No fibrils were

observed for the 45-54W peptide in the absence of α-syn. The control peptide 71-82W as well as the wild-type 45-54 sequence had no effect upon fibril formation (Figures 3e-f) supporting α-syn specificity for the 45-54W peptide.

Circular Dichroism demonstrates a large reduction in β-sheet content – Since amyloid fibrils are predominately *β*-sheet, we also used CD spectroscopy to provide structural characterisation of the aggregates through the ThT continuous growth experiments. The data presented in Figure 4a show spectra over 17 time points of the continuous growth assay. A single negative peak at 218nm develops across the time course along with the loss of minima at ~200nm, consistent with the gain of *β*-sheet structure and the loss of a random coil. As predicted from the ThT data above the *β*-structure did not form for the α-syn incubated with 45-54W at a 1:1 stoichiometry sample (Figure 4b). In addition, the minima at ~200nm did not significantly diminish. A similar spectrum was observed for 45-54W alone (i.e 0:1 stoichiometry) after 75 hours of incubation, indicating that this peptide does not aggregate in isolation. The lack of CD signal intensity at 218nm for α-syn incubated with the 45-54W peptide is unlikely to be attributed to increased aggregation or precipitation. This is because any peptides causing increased precipitation would also generate large increases in ThT binding and would be clearly observed in AFM imaging experiments. Neither the wild-type 45-54 α-syn sequence nor the 71-82W had any effect upon the conversion to the *β*-structure (Figure 4c-d), again demonstrating α-syn specificity for the 45-54W peptide.

MTT studies demonstrate reduced amyloid toxicity to cells – MTT ((3-(4,5-Dimethylthiazol-2-yl)-2,5-diphenyltetrazolium bromide)) cell toxicity experiments were performed using Rat phaeochromocytoma (PC12) neuronal-like cells to assess toxicity of α-syn and the preventative effects of the 45-54W peptide generated in this study. MTT assays (Figure 5a) were performed at a α-syn : 45-54W ratio of 1:1 and presented as raw A_{570} signal. At this stoichiometry, 45-54W improved cell viability by 65-85% relative to α-syn in isolation. Dose dependency experiments demonstrated that at molar ratios of 1:0.01 or 1:0.1 there was no effect on toxicity. At 1:0.5 the recovery was improved, maximizing at 1:1 and becoming less pronounced at increasingly higher molar ratios (Figure 5b). In addition, MTT experiments using samples taken throughout the continuous growth experiment demonstrated that α-syn becomes progressively more toxic with time and is most toxic within the stationary phase of fibril growth (Figure 5c). As predicted from ThT, CD and AFM experiments, MTT experiments using 45-54wt or 71-82W demonstrate that although these peptides are not toxic in isolation, they have very little effect upon α-syn toxicity (Figure 5d). Finally, increasing concentrations of 45-54W in isolation demonstrate that it is not toxic.

SDS-PAGE analysis demonstrates that 45-54W is able to interact with α-syn and lower oligomeric state – A range of samples were taken from the endpoint (75 h) of continuous growth experiments and subjected to ADS-PAGE analysis (Figure 6). Two clear bands at ~40 KDa and ~60 KDa (as determined by graph analysis of log MW vs. relative migration distance; data not shown) were found to be present within the 1:0 sample as well as 1:0.01, 1:0.1, 1:2 and to a lesser extent the 1:5 sample, suggesting the presence of α-syn trimers (40/14.5 = 2.8) and tetramers (60/14.5 = 4.1). No bands corresponding to dimers or 5-8mers were observed. At a molar ratio of 1:1 or higher these bands were found to absent and are replaced by the presence three low molecular weight bands. One band at ~15 KDa may represent the α-syn:45-54W complex. The second and third bands are below the resolution limit of the gel but are likely to represent momomeric α-syn (14.5 KDa) and the inhibitor alone (1 KDa). NAlthough under denaturing conditions (which therefore precludes more detailed interpretation), this experiment demonstrates that 45-54W is able to interact with α-syn and lower the oligomeric state, possibly to the momomer.

DISCUSSION

In conclusion, we have employed semi-rational design combined with intracellular PCA to demonstrate this as an effective methodology for developing α-syn aggregation antagonists.

To date, the majority of *β*-sheet breaker compounds are either designed to target or are based specifically on the 71-82 region of the protein, since this is known to aggregate in isolation and therefore thought to be responsible for instigating amyloidosis of the parent protein. Inhibitors include N-methylated derivatives of the same sequence (9), single chain antibodies (31), and small molecule compounds such as curcumin (32) and epigallocatechin gallate (33).

In contrast, our approach has focused on the development of a library centered on the 45-54 region in which four of the five known α-syn familial mutants implicated in early onset PD are found. All of the known mutations in this region result in either increased α-syn aggregation rates or increased numbers of oligomers and therefore increased levels of toxicity. All residues in the 45-54 sequence were therefore scrambled to give two, three, or six options, giving rise to a library of 209,952 members (See Figure 1). This was constructed to include all wild-type options as well as the mutations found in E46K, A53T and H50Q respectively. Half of the ten positions re-selected the wild-type residues while the remaining five resulted in new selections. These were E46D, V48I, H50N, A53K and T54A. In amyloid inhibition experiments (i.e. inhibitor and monomeric α-syn mixed at time zero and amyloid growth continuously monitored) and at a stoichiometry of 1:1, we observe that the classical sigmoidal amyloid growth for an inhibitor free (1:0) sample is abolished. Rather, the signal is held at ~8% of the signal observed in the stationary phase of the 1:0 sample. At a stoichiometry of 1:0.5 amyloid growth is significantly slower, taking approximately twice as long for the fluorescence intensity to match that of the 1:0 sample. In accordance with an expected dose dependency, at 1:0.1 stoichiometry or lower the inhibitory effect is lost. The impressive efficacy of the 1:1 sample in continuous growth ThT experiments is supported by both CD data which show that the conversion from a random-coil like structure consistent with native α-syn to a classical amyloid *β*-sheet signal does not occur in the 1:1 sample, and MTT data which show that toxicity associated with a-syn aggregation is almost completely reversed in the presence of 45-54W. Moreover, a clear reduction to almost no fibrils is observed by direct AFM imaging. This is corroborated by SDS-PAGE experiments that shows the loss of low molecular weight oligomers in the presence of 45-54W at 1:1 stoichiometry or higher.

We have designed a library based on the 45-54 region of wild-type α-syn, and have created a potent peptide inhibitor of aggregation. In the future nit may be possible to derive more potent inhibitors of the mutagenic versions of α-syn that are in-turn more effective with the wild-type protein. Not only does this point towards a new target for the design of new inhibitors, the peptide derived here using PCA has the potential itself to be modified into drugs to slow or even prevent the onset of Parkinson's disease.

ACKNOWLEDGEMENT

The authors acknowledge the use made of the Park Systems XE-120 Atomic Force Microscope which was on loan from the EPSRC (Engineering and Physical Sciences Research Council) Engineering Instrument Pool. The authors wish to thank Dr Miao Yu for excellent technical support. H.C., N.M.K., and J.M.M. thank Parkinson's UK for awarding a PhD Studentship (H-1001). J.M.M holds a Cancer Research UK Career Establishment Award (A11738).

REFERENCES

1. Fink, A. L. (2006) The aggregation and fibrillation of alpha-synuclein. *Acc Chem Res* **39**, 628-634

2. Cookson, M. R. (2009) alpha-Synuclein and neuronal cell death. *Mol Neurodegener* **4**, 9

3. Irvine, G. B., El-Agnaf, O. M., Shankar, G. M., and Walsh, D. M. (2008) Protein aggregation in the brain: the molecular basis for Alzheimer's and Parkinson's diseases. *Mol Med* **14**, 451-464

4. Outeiro, T. F., Putcha, P., Tetzlaff, J. E., Spoelgen, R., Koker, M., Carvalho, F., Hyman, B. T., and McLean, P. J. (2008) Formation of toxic oligomeric alpha-synuclein species in living cells. *PLoS One* **3**, e1867

5. Giasson, B. I., Murray, I. V., Trojanowski, J. Q., and Lee, V. M. (2001) A hydrophobic stretch of 12 amino acid residues in the middle of alpha-synuclein is essential for filament assembly. *J Biol Chem* **276**, 2380-2386

6. Madine, J., Doig, A. J., Kitmitto, A., and Middleton, D. A. (2005) Studies of the aggregation of an amyloidogenic alpha-synuclein peptide fragment. *Biochem Soc Trans* **33**, 1113-1115

7. Periquet, M., Fulga, T., Myllykangas, L., Schlossmacher, M. G., and Feany, M. B. (2007) Aggregated alpha-synuclein mediates dopaminergic neurotoxicity in vivo. *J Neurosci* **27**, 3338-3346

8. El-Agnaf, O. M., Paleologou, K. E., Greer, B., Abogrein, A. M., King, J. E., Salem, S. A., Fullwood, N. J., Benson, F. E., Hewitt, R., Ford, K. J., Martin, F. L., Harriott, P., Cookson, M. R., and Allsop, D. (2004) A strategy for designing inhibitors of alpha-synuclein aggregation and toxicity as a novel treatment for Parkinson's disease and related disorders. *FASEB J* **18**, 1315-1317

9. Madine, J., Doig, A. J., and Middleton, D. A. (2008) Design of an N-methylated peptide inhibitor of alpha-synuclein aggregation guided by solid-state NMR. *J Am Chem Soc* **130**, 7873-7881

10. Lesage, S., Anheim, M., Letournel, F., Bousset, L., Honore, A., Rozas, N., Pieri, L., Madiona, K., Durr, A., Melki, R., Verny, C., and Brice, A. (2013) G51D alpha-synuclein mutation causes a novel parkinsonian-pyramidal syndrome. *Ann Neurol* **73**, 459-471

11. Bussell, R., Jr., and Eliezer, D. (2001) Residual structure and dynamics in Parkinson's disease-associated mutants of alpha-synuclein. *J Biol Chem* **276**, 45996-46003

12. Greenbaum, E. A., Graves, C. L., Mishizen-Eberz, A. J., Lupoli, M. A., Lynch, D. R., Englander, S. W., Axelsen, P. H., and Giasson, B. I. (2005) The E46K mutation in alpha-synuclein increases amyloid fibril formation. *J Biol Chem* **280**, 7800-7807

13. Ghosh, D., Mondal, M., Mohite, G. M., Singh, P. K., Ranjan, P., Anoop, A., Ghosh, S., Jha, N. N., Kumar, A., and Maji, S. K. (2013) The Parkinson's disease-associated H50Q mutation accelerates alpha-Synuclein aggregation in vitro. *Biochemistry* **52**, 6925-6927

14. Rutherford, N. J., Moore, B. D., Golde, T. E., and Giasson, B. I. (2014) Divergent effects of the H50Q and G51D SNCA mutations on the aggregation of alpha-synuclein. *J Neurochem*

15. Pelletier, J. N., Campbell-Valois, F. X., and Michnick, S. W. (1998) Oligomerization domain-directed reassembly of active dihydrofolate reductase from rationally designed fragments. *Proc Natl Acad Sci U S A* **95**, 12141-12146

16. Mason, J. M., Schmitz, M. A., Muller, K. M., and Arndt, K. M. (2006) Semirational design of Jun-Fos coiled coils with increased affinity: Universal implications for leucine zipper prediction and design. *Proc Natl Acad Sci U S A* **103**, 8989-8994

17. Acerra, N., Kad, N. M., Cheruvara, H., and Mason, J. M. (2014) Intracellular Selection of peptide Inhibitors that Target Disulphide-Bridged Abeta42 Oligomers. *Protein Science* **23**, 1262-1274

18. Acerra, N., Kad, N. M., and Mason, J. M. (2013) Combining Intracellular Selection with Protein-fragment Complementation to Derive Aβ interacting Peptides. *Protein Eng Des Sel* **26**, 463-470

19. Butt, T. R., Edavettal, S. C., Hall, J. P., and Mattern, M. R. (2005) SUMO fusion technology for difficult-to-express proteins. *Protein Expr Purif* **43**, 1-9

20. Fields, G. B., and Noble, R. L. (1990) Solid-Phase Peptide-Synthesis Utilizing 9-Fluorenylmethoxycarbonyl Amino-Acids. *Int J Pept Prot Res* **35**, 161-214

21. Maurer-Stroh, S., Debulpaep, M., Kuemmerer, N., Lopez de la Paz, M., Martins, I. C., Reumers, J., Morris, K. L., Copland, A., Serpell, L., Serrano, L., Schymkowitz, J. W., and Rousseau, F. (2010) Exploring the sequence determinants of amyloid structure using position-specific scoring matrices. *Nat Methods* **7**, 237-242

22. Frousios, K. K., Iconomidou, V. A., Karletidi, C. M., and Hamodrakas, S. J. (2009) Amyloidogenic determinants are usually not buried. *BMC Struct Biol* **9**, 44

23. Trovato, A., Seno, F., and Tosatto, S. C. (2007) The PASTA server for protein aggregation prediction. *Protein Eng Des Sel* **20**, 521-523

24. Tartaglia, G. G., and Vendruscolo, M. (2008) The Zyggregator method for predicting protein aggregation propensities. *Chem Soc Rev* **37**, 1395-1401

25. Fernandez-Escamilla, A. M., Rousseau, F., Schymkowitz, J., and Serrano, L. (2004) Prediction of sequence-dependent and mutational effects on the aggregation of peptides and proteins. *Nat Biotechnol* **22**, 1302-1306

26. Kad, N. M., Myers, S. L., Smith, D. P., Smith, D. A., Radford, S. E., and Thomson, N. H. (2003) Hierarchical assembly of beta2-microglobulin amyloid in vitro revealed by atomic force microscopy. *J Mol Biol* **330**, 785-797

27. Shearman, M. S., Ragan, C. I., and Iversen, L. L. (1994) Inhibition of PC12 cell redox activity is a specific, early indicator of the mechanism of beta-amyloid-mediated cell death. *Proc Natl Acad Sci U S A* **91**, 1470-1474

28. Hughes, E., Burke, R. M., and Doig, A. J. (2000) Inhibition of toxicity in the beta-amyloid peptide fragment beta -(25-35) using N-methylated derivatives: a general strategy to prevent amyloid formation. *J Biol Chem* **275**, 25109-25115

29. Pike, C. J., Walencewicz-Wasserman, A. J., Kosmoski, J., Cribbs, D. H., Glabe, C. G., and Cotman, C. W. (1995) Structure-activity analyses of beta-amyloid peptides: contributions of the beta 25-35 region to aggregation and neurotoxicity. *J Neurochem* **64**, 253-265

30. Hung, L. W., Ciccotosto, G. D., Giannakis, E., Tew, D. J., Perez, K., Masters, C. L., Cappai, R., Wade, J. D., and Barnham, K. J. (2008) Amyloid-beta peptide (Abeta) neurotoxicity is modulated by the rate of peptide aggregation: Abeta dimers and trimers correlate with neurotoxicity. *J Neurosci* **28**, 11950-11958

31. Emadi, S., Liu, R., Yuan, B., Schulz, P., McAllister, C., Lyubchenko, Y., Messer, A., and Sierks, M. R. (2004) Inhibiting aggregation of alpha-synuclein with human single chain antibody fragments. *Biochemistry* **43**, 2871-2878

32. Singh, P. K., Kotia, V., Ghosh, D., Mohite, G. M., Kumar, A., and Maji, S. K. (2013) Curcumin modulates alpha-synuclein aggregation and toxicity. *ACS Chem Neurosci* **4**, 393-407

33. Bieschke, J., Russ, J., Friedrich, R. P., Ehrnhoefer, D. E., Wobst, H., Neugebauer, K., and Wanker, E. E. (2010) EGCG remodels mature alpha-synuclein and amyloid-beta fibrils and reduces cellular toxicity. *Proc Natl Acad Sci U S A* **107**, 7710-7715

FIGURE LEGENDS

Figure 1: ***a)*** shown are residues 45-54 of wild-type α-syn (KEGVVHGVAT) as well as the three well studied point mutation sites (46, 50 and 53). Degenerate codons for library construction are shown below (R=A/G, V=A/C/G, W=A/T, B=C/G/T, and H=A/C/T). ***b)*** shown are amino acid options at each position to generate a 209,952 member peptide library. The wild-type residue options (top line) as well as alternative options, including those point mutations associated with early onset PD (shown in bold) were also considered in the library design. ***c)*** The winner peptide (KDGIVNGVKA) emerged from single step selection followed by two rounds of competition selection PCA.

Figure 2: ***a)*** Protein-fragment Complementation Assay: Peptide library members that bind to wild-type α-syn$_{1\text{-}140}$ recombine murine DHFR and lead to colonies under selective conditions (bacterial DHFR is specifically inhibited using trimethoprim). Those peptides that bind with highest affinity to the α-syn target are able to confer cell growth by i) reconstituting mDHFR to restore activity and ii) reducing the toxicity associated with any given oligomeric amyloid state. In competition selection, subsequent passages in liquid media isolate potential winners with highest efficacy. Since PCA is performed in the cytoplasm of *E.coli*, the non-specific, unstable, aggregation prone (insoluble), protease susceptible members are removed. ***b)*** DNA sequencing results of library pools for passages 0-6. Both single step selection (P0) and competition selection (P1, P2 and P6) are shown. The peptide sequence KDGIVNGVKA was seen to dominate from P2 onwards.

Figure 3 ***a)*** Continuous ThT growth: The data shows a significant reduction in ThT signal (~92%) at a 1:1 stoichiometry. The ThT signal at a molar ratio of 1:0.5 shows that the amyloid growth rate is significantly reduced compared to wild-type. At increasingly sub-stoichiometric ratios, the ThT fluorescence indicates reduced peptide activity in an expected dose dependent manner. Peptide 45-54W alone (0:1) shows no ThT binding indicating that it does not aggregate in isolation. Aliquots of samples were collected at 17 different time points for 1:0 (lag phase: T0, T1; exponential phase: T3, T7, T14 and stationary phase: End are shown) and 3 time points for 1:1 (T0, T1 and End) for further analysis using AFM and CD. ***b)*** AFM images showing the endpoint samples (75 hours) for all stoichiometries used in continuous ThT growth experiments. A considerable reduction in fibril load is observed at a molar ratio

of 1:1. All other stoichiometries showed no major reduction of amyloid content relative to 1:0. The 45-54W peptide (0:1) demonstrates that this peptide does not aggregate in isolation. ***c)*** AFM images showing the gradual increase of amyloid content along various time points for 1:0. Shown are six samples (T0-T16) taken taken from lag, exponential and stationary phase. The time points these were T0=0 hr, T1=10 hrs, T3=33.3hrs, T7=37.5 hrs, T14=49 hrs and End=75 hrs. ***d)*** A large reduction in amyloid content was observed for the for 1:1 sample with 45-54W. For these images T0=0 hr, T1= 37.5 hrs and T2= 75 hrs. ***e)*** No reduction in amyloid content was observed for the 1:1 sample with wild-type 45-54. For these images T0=0 hr, T1= 33.75 hrs and T2= 75 hrs. ***f)*** No reduction in amyloid content was observed for for 1:1 sample with 71-82W. For these images T0=0 hr, T1= 28.75 hrs and T2= 75 hrs. For all samples, many numbers of images were taken at each time point in order to confirm the morphology and number of fibrils present in each image.

Figure 4 ***a)*** CD spectra using the same samples used in ThT and AFM experiments. Shown is the gradual development of a minima at 218nm across the time course along with the loss of a minima at 200nm, consistent with the gain of β-sheet structure and the loss of a random coil in the 1:0 sample. ***b)*** In the 1:1 samples, the minima at ~200 nm was prominent even after 75 hours of incubation with no development of a 218 nm signal, confirming the efficacy of the 45-54W peptide in preventing the formation of β-sheet structure. A similar spectrum was obtained for the peptide 45-54W (0:1), confirming that the peptide does not adopt a β-sheet structure in isolation. ***c)*** A 1:1 sample with the 45-54 wild-type sequence had no effect upon the conversion on β-sheet structure and the loss of a random coil. The 45-54 wild-type sequence in isolation (0:1) did not adopt a β-sheet structure in isolation. ***d)*** Similarly, a PCA derived peptide based on the 71-82 region of α-syn had no effect upon the conversion on β-sheet structure and the loss of a random coil. Again the 71-82W sequence in isolation (0:1) did not adopt a β-sheet structure in isolation.

Figure 5 MTT cytotoxicity assays using rat pheochromocytoma (PC12) cells, α-syn, and the inhibitory effect of 45-54W peptide on α-syn aggregation. ***a)*** Shown from left to right are i) PC12 cells only, ii) PC12 cells plus buffer, iii) PC12 cells plus buffer and ThT, iv) PC12 cells plus α-syn (5uM) in buffer, v) PC12 cells plus α-syn (5uM) in buffer plus ThT and vi) α-syn with 45-54W at a 1:1 stoichiometry. The latter leads to a large restoration of activity (~85%). ***b)*** Increasing molar ratios of α-syn:45-54W

demonstrates a dose dependency. Samples are taken from the endpoint of the continuous growth experiment (75 h) and show that no effect upon toxicity is observed at 1:0.01 or 1:0.1 and that a molar ratio of 1:0.5 is needed to partially rescue the cells (~28% recovery) from the cytotoxic effect of α-syn. This increases at 1:1 (~63%) and becomes progressively less pronounced at increasingly higher molar ratios. ***c)*** The effect of incubation time on toxicity using samples taken directly from the continuous growth experiment. Results demonstrate that toxicity progressively increases as the sample ages and is at its maximum within the stationary phase of the continuous growth. ***d)*** Increasing concentrations of 45-54W demonstrates that the peptide in isolation is not toxic to PC12 cells. MTT experiments using 45-54wt (bold surround) or 71-82W (hashed surround) demonstrate that the peptide are not toxic in isolation but at a ratio of 1:1 with α-syn have almost no effect upon toxicity. All experiments were undertaken in triplicate and errors are shown as the standard deviation.

Figure 6: SDS-PAGE analysis shows a range of samples taken from the endpoint (75 h) of continuous growth experiments. Two clear bands at ~40 KDa and ~60 KDa (as determined by graph analysis of log MW vs. relative migration distance) are present within the 1:0 sample as well as 1:0.01, 1:0.1, 1:2 and 1:5 samples, suggesting the presence of α-syn trimers (40/14.5 = 2.8) and tetramers (60/14.5 = 4.1). At molar ratios of 1:1 or higher these bands are absent and are replaced by the presence three low molecular weight bands. One band at ~15 KDa may represent the α-syn:45-54W complex. The second and third bands are below the resolution limit of the gel but are likely to represent momomeric α-syn (14.5 KDa) and the inhibitor alone (1 KDa).

Figure 1

a)

^{45}**K**	^{46}**E**	^{47}**G**	^{48}**V**	^{49}**V**	^{50}**H**	^{51}**G**	^{52}**V**	^{53}**A**	^{54}**T**
RAA	VAW	GBG	VTT	VTT	VAW	GBG	VTT	**RHA**	RCC

b)

K	E	G	V	V	H	G	V	A	T
E	Q	A	I	I	**Q**	A	I	V	A
	N	V	L	L	N	V	L	**T**	
	K				K			I	
	D				D			K	
	H				E			E	

(2*6*3*3*3*6*3*3*6*2 = 209,952 member library)

c)

K	**D**	**G**	**I**	**V**	**N**	**G**	**V**	**K**	**A**

Figure 2

a) PCA

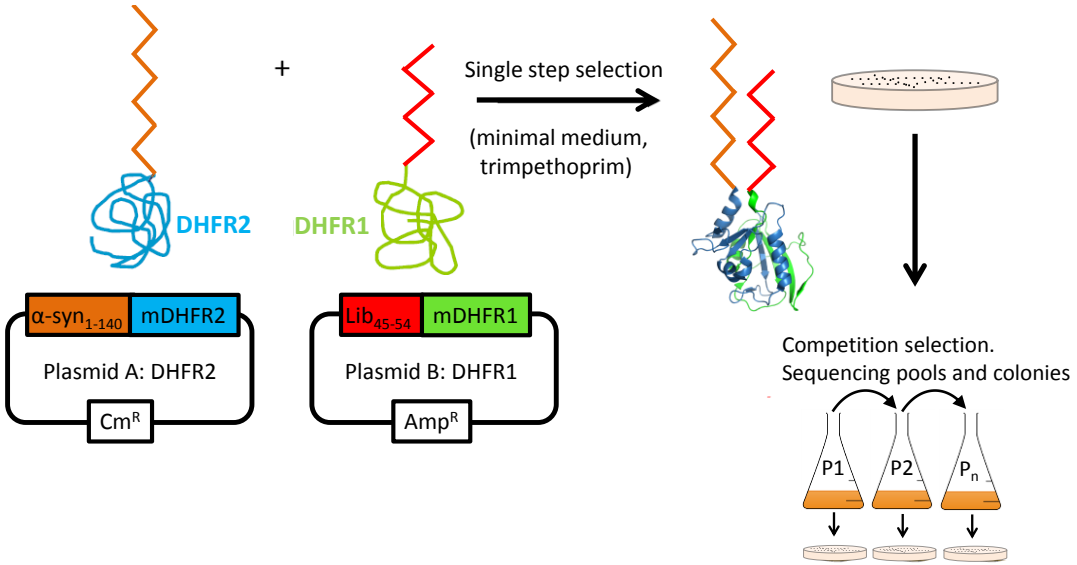

b) DNA sequencing

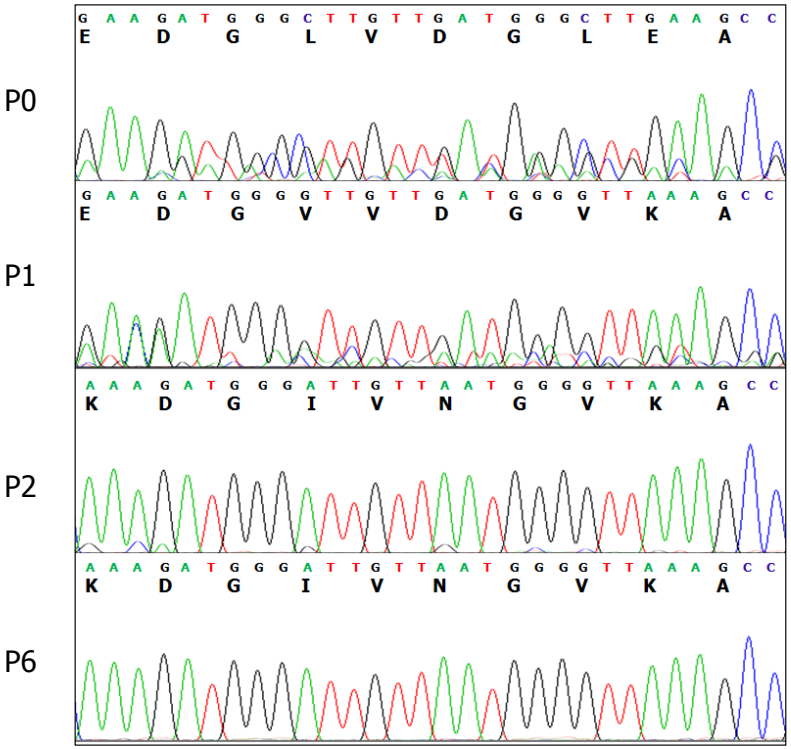

Figure 3a

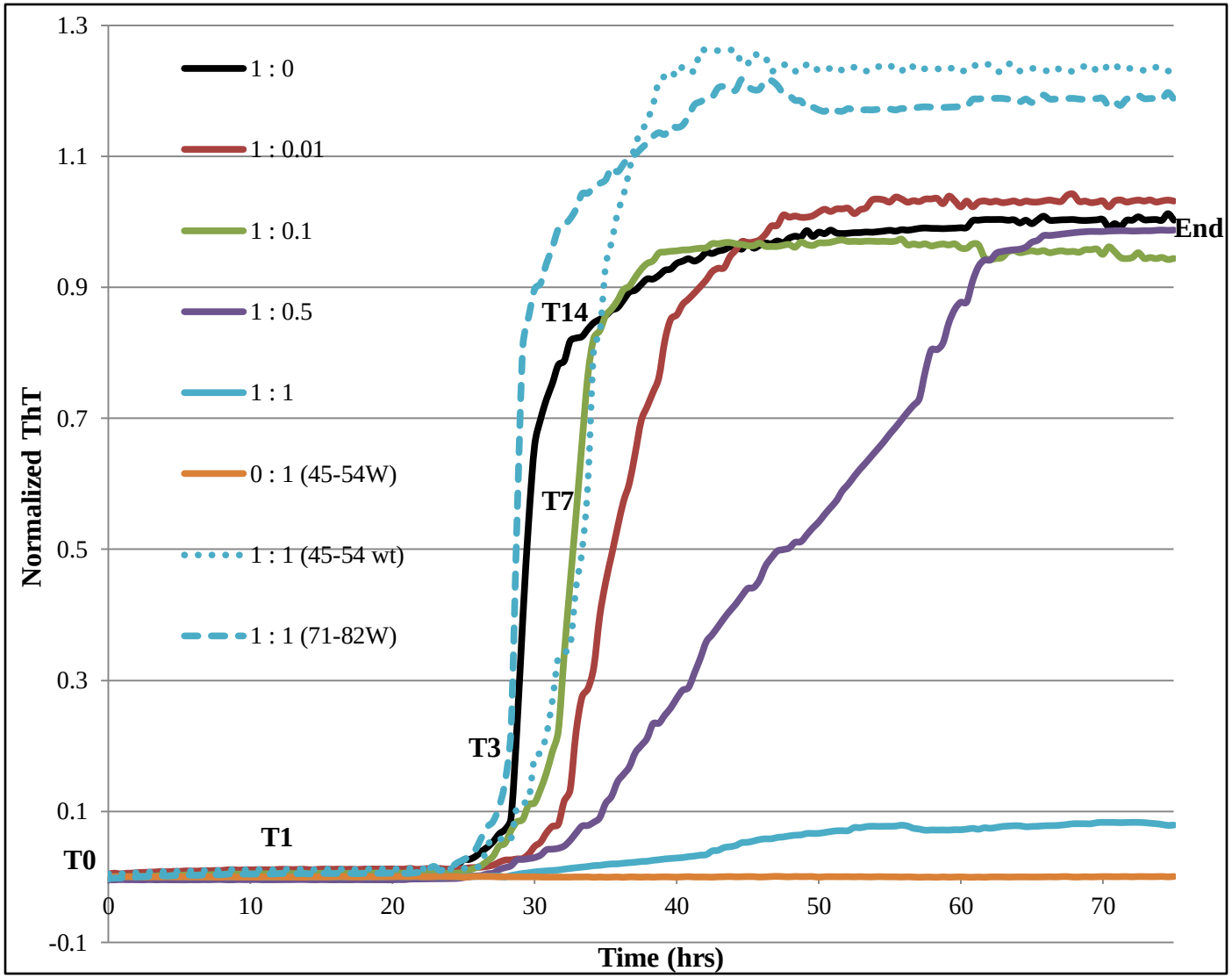
1.3
1.1
0.9
0.7
0.5
0.3
0.1
-0.1
0
10
20
30
40
50
60
70
Normalized ThT
Time (hrs)
1 : 0
1 : 0.01
1 : 0.1
1 : 0.5
1 : 1
0 : 1 (45-54W)
1 : 1 (45-54 wt)
1 : 1 (71-82W)
T0
T1
T3
T7
T14
End

Figure 3

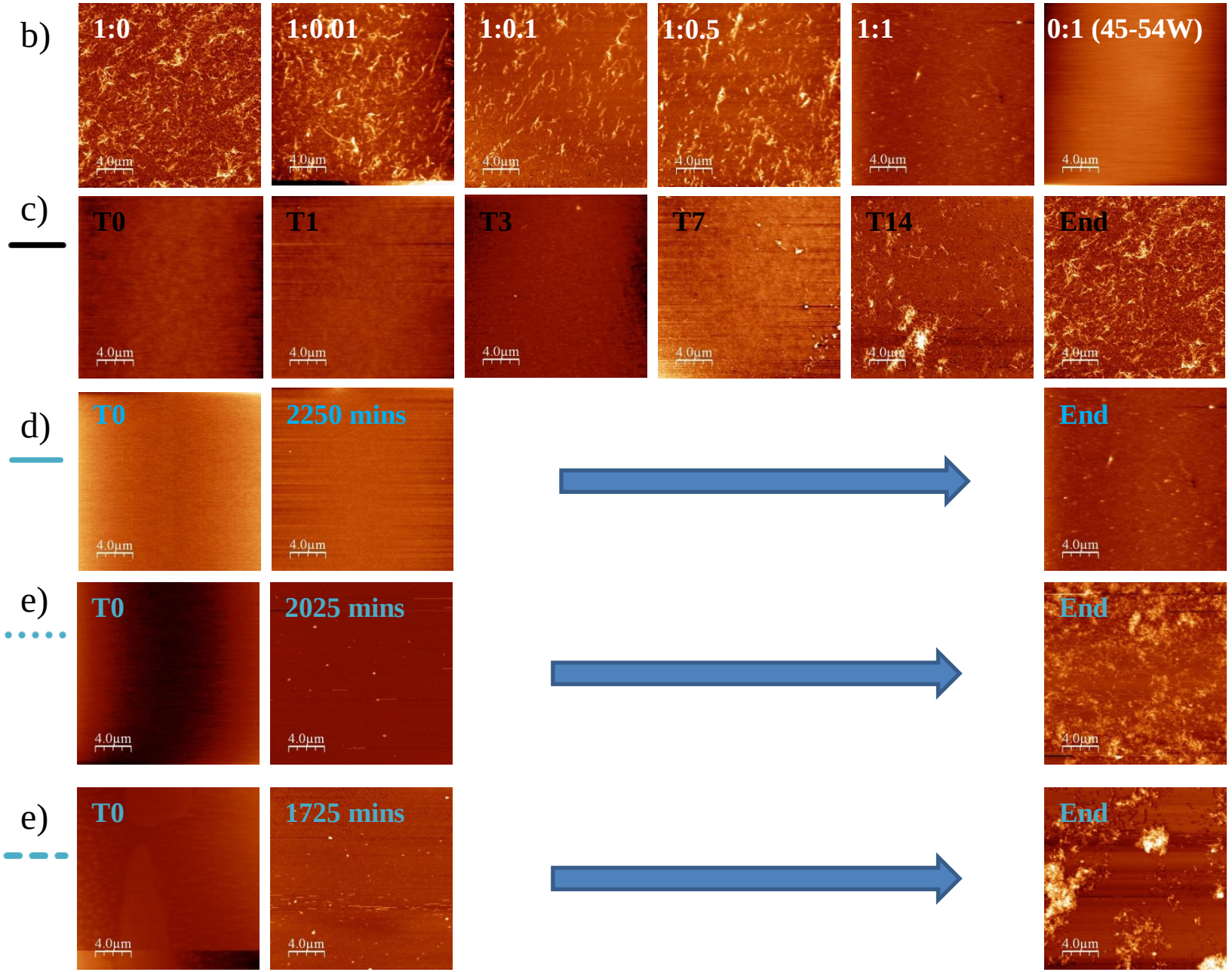
b)
1:0
1:0.01
1:0.1
1:0.5
1:1
0:1 (45-54W)
c)
T0
T1
T3
T7
T14
End
d)
T0
2250 mins
End
e)
T0
2025 mins
End
e)
T0
1725 mins
End
4.0µm

Figure 4

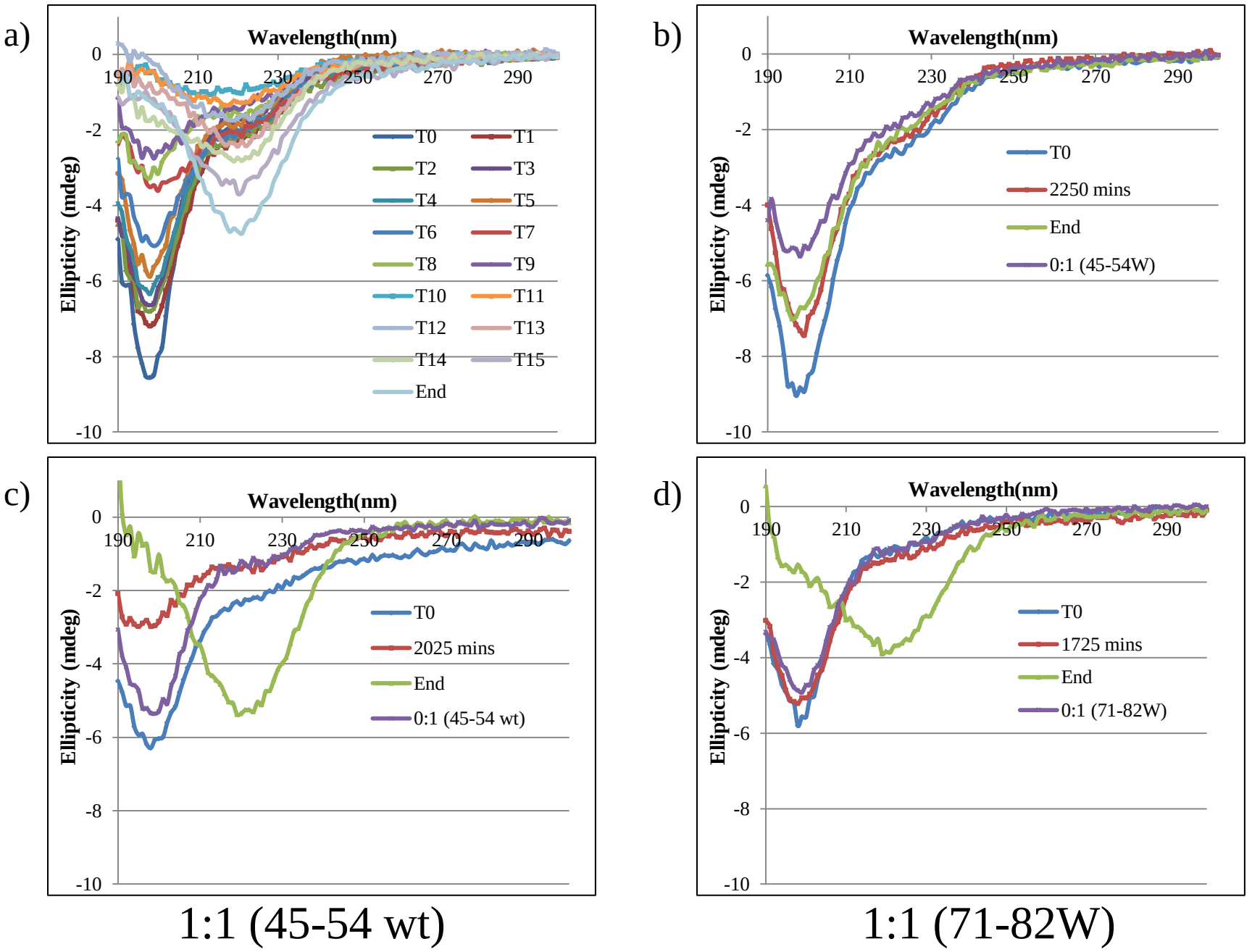
a)
1:0
Wavelength(nm)
Ellipticity (mdeg)
T0
T1
T2
T3
T4
T5
T6
T7
T8
T9
T10
T11
T12
T13
T14
T15
End
b)
1:1 (45-54W)
T0
2250 mins
End
0:1 (45-54W)
c)
1:1 (45-54 wt)
T0
2025 mins
End
0:1 (45-54 wt)
d)
1:1 (71-82W)
T0
1725 mins
End
0:1 (71-82W)

Figure 5

a)

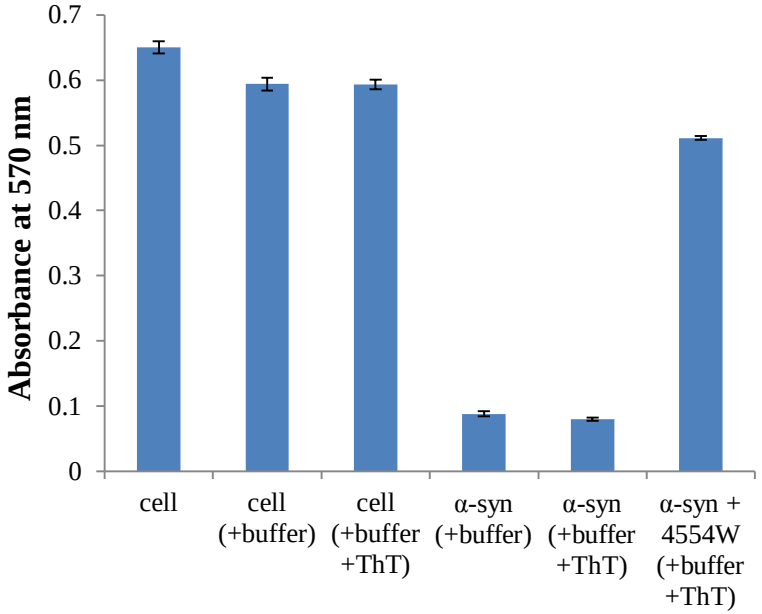
Absorbance at 570 nm
0.7
0.6
0.5
0.4
0.3
0.2
0.1
0
cell
cell (+buffer)
cell (+buffer +ThT)
α-syn (+buffer)
α-syn (+buffer +ThT)
α-syn + 4554W (+buffer +ThT)

b)

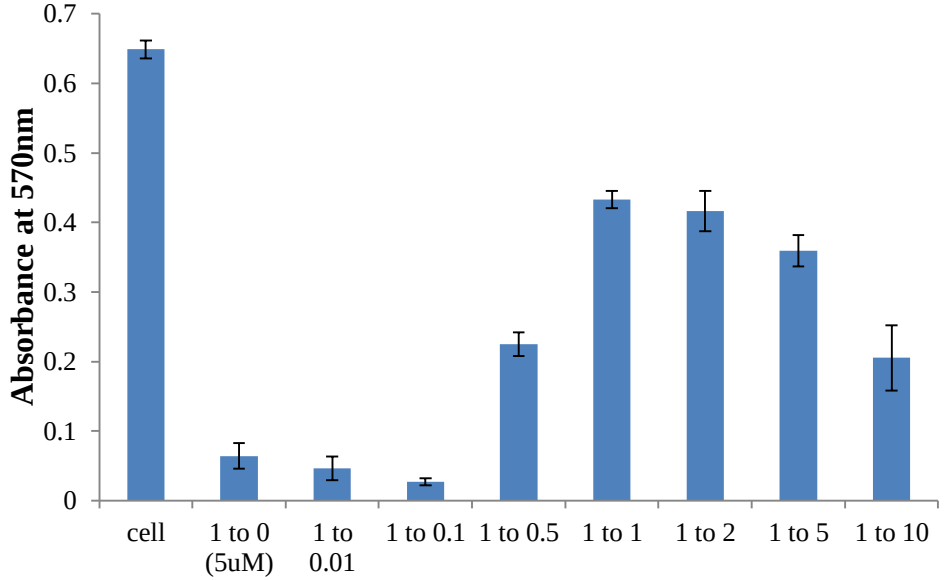
Absorbance at 570nm
0.7
0.6
0.5
0.4
0.3
0.2
0.1
0
cell
1 to 0 (5uM)
1 to 0.01
1 to 0.1
1 to 0.5
1 to 1
1 to 2
1 to 5
1 to 10

Figure 5

c)

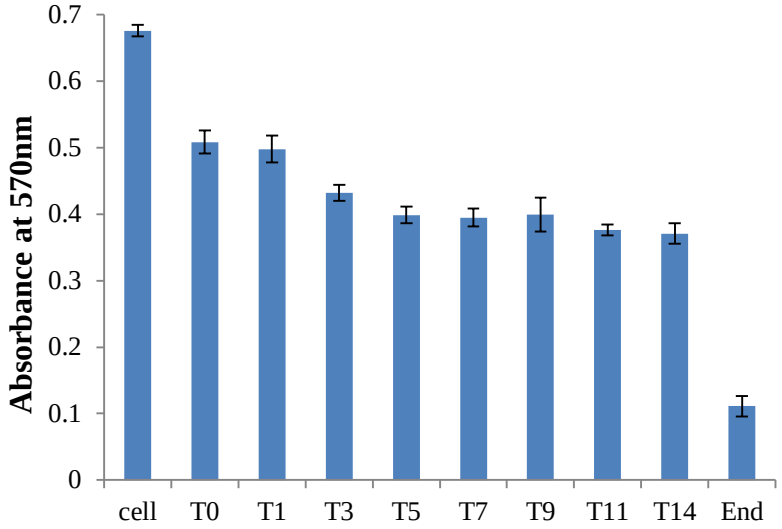
Absorbance at 570nm
0.7
0.6
0.5
0.4
0.3
0.2
0.1
0
cell
T0
T1
T3
T5
T7
T9
T11
T14
End

d)

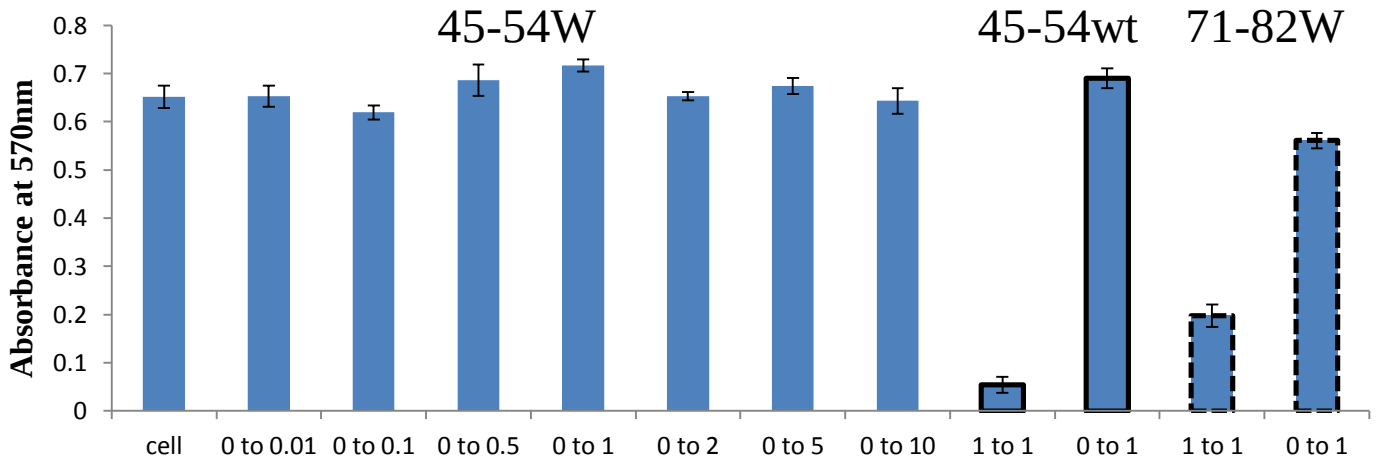
45-54W
45-54wt
71-82W
Absorbance at 570nm
0.8
0.7
0.6
0.5
0.4
0.3
0.2
0.1
0
cell
0 to 0.01
0 to 0.1
0 to 0.5
0 to 1
0 to 2
0 to 5
0 to 10
1 to 1
0 to 1
1 to 1
0 to 1

Figure 6

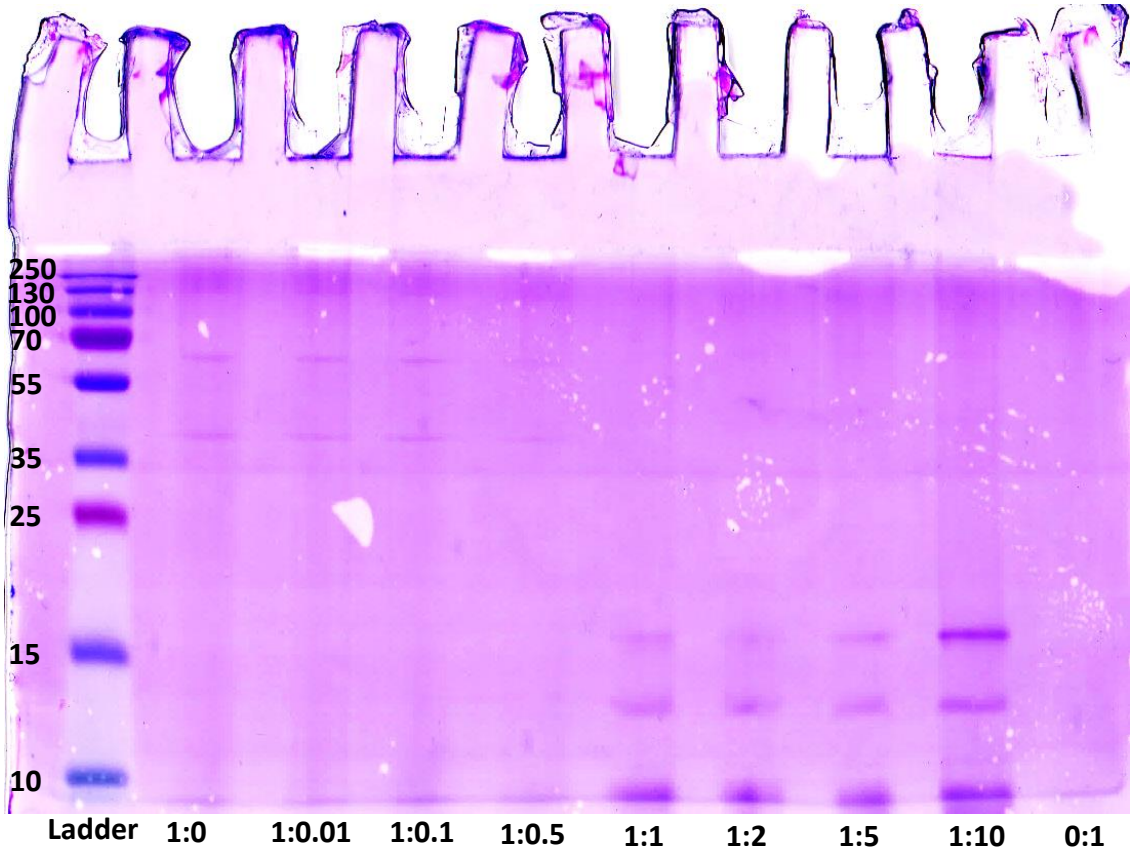
250
130
100
70
55
35
25
15
10
Ladder
1:0
1:0.01
1:0.1
1:0.5
1:1
1:2
1:5
1:10
0:1